Hydroxamate-Bridged Dinuclear Nickel Complexes as Models for Urease Inhibition†

M. Arnold,‡ David A. Brown,*,§ O. Deeg,‡ W. Errington,|| W. Haase,⊥ K. Herlihy,§,# T. J. Kemp,|| H. Nimir,§ and R. Werner⊥

Department of Chemistry, University College, Belfield, Dublin 4, Ireland, Department of Chemistry, University of Warwick, Coventry, CV4 7AL, U.K., and Institut für Physikalische Chemie, Technische Universität, Darmstadt, Germany

Received September 10, 1997

Facile reaction of the model urease complex $[Ni_2(OAc)_3(urea)(tmen)_2][OTf]$ **(A)** with acetohydroxamic acid (AHA) gives the monobridged hydroxamate complex **(I)** $[Ni_2(OAc)_2(AA)(urea)(tmen)_2][OTf]$ with a Ni−Ni distance of 3.434(1) Å compared to that of 3.5 Å in urease (OAc, CH_3COO^-; tmen, *N*,*N*,*N*′,*N*′-tetramethylethylenediamine; OTf, CF_3SO_3; AHA, acetohydroxamic acid; AA, acetohydroxamate anion). **I** is a close model of one proposed mode of urease inhibition by hydroxamic acids, recently observed in the acetohydroxamate-inhibited C319A variant of *Klebsiella aerogenes* urease. Reaction of $[Ni_2(OH_2)(OAc)_4(tmen)_2]$ **(B)** with AHA gives the dibridged hydroxamate complex **(II)** $[Ni_2(OAc)(AA)_2(tmen)_2][OAc]$ with a Ni−Ni distance of 3.005(1) Å. Infrared spectroscopic studies provide evidence for the bridging acetate groups undergoing carboxylate shifts thereby assisting replacement of acetate by hydroxamate. Both **I** and **II** show ferromagnetic exchange coupling.

Introduction

Urease catalyses the hydrolysis of urea to ammonia and carbamate and subsequently to carbon dioxide and ammonia and is central to the virulence of *Proteus mirabilis* and *Helicobacter pylori*.[1] The generally accepted mechanism for urea hydrolysis was proposed by Zerner[2] in which a hydroxide ion coordinated to one nickel site of a dinuclear nickel center attacks the carbonyl C atom of the urea substrate coordinated via its oxygen atom to the other nickel site of the dinickel center to form a bridged tetrahedral intermediate. This mechanism is consistent with the recently determined crystal structure of urease from *Klebsiella aerogenes*[3] at 2.2 Å resolution which confirmed the presence of a dinickel site in urease with a Ni−Ni distance of 3.5 Å bridged by a carboxylate function of a carbamylated lysine residue. In this structure, the coordination of Ni-1 is pseudotetrahedral involving two histidine nitrogens, an oxygen of the bridging carbamylated lysine residue, and a weak interaction with a water molecule (Wat-1 in ref 3) which is primarily coordinated to Ni-2. Ni-2 is distorted trigonal pyramidal involving nitrogen coordination by two different histidines from those bonded to Ni-1, the other bridging carbamate oxygen, an aspartate oxygen, and Wat-1. However, recent crystal structure determinations of Cys 319 variants[4] and the model for wild-type ureases indicate three water positions:

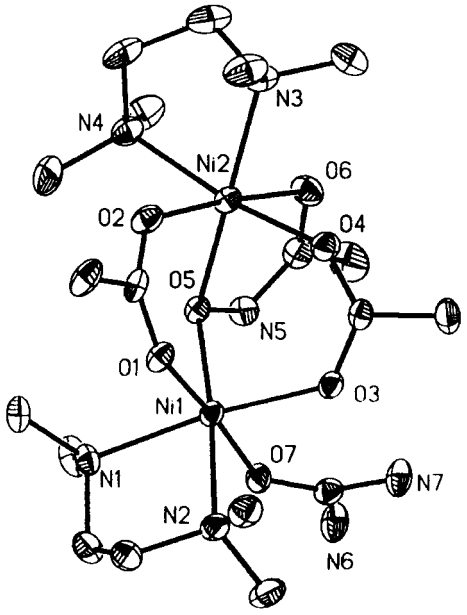

Figure 1. Molecular structure of the cation in compound **I** showing the labeling scheme. All hydrogens have been omitted for clarity.

Wat-500 which bridges the two nickel centers, Ni-1 and Ni-2, Wat-501 binding to Ni-1, and Wat-502 (Wat-1 above in ref 3) binding to Ni-2. Urease is inhibited by a variety of agents including thiols[5] and hydroxamic acids.[6] One suggested mode of inhibition involves coordination of the inhibitor to only one nickel center while another involves the inhibitor bridging the dinickel center.[6] Recently, Pecoraro et al.[7] reported the crystal structure of a dinuclear nickel complex containing *two* bridging salicylhydroxamate bridges with a Ni−Ni distance of 3.016 Å and suggested that inhibited urease would have only *one* bridging hydroxamate.

* Author for correspondence.

† Dedicated to Professor Achim Müller, University of Bielefeld, Germany, on the occasion of his 60th birthday.

‡ Erasmus student, University of Wurzburg, Germany.
§ University College.
|| University of Warwick.
⊥ Technische Universität.
Present address: Department of Physics, Emory University, Atlanta, GA.

(1) Mobley H. L. T.; Island M. O.;Hausinger R. P. *Microbiol. Rev.* **1995**, *59*, 451.
(2) Dixon, N. E.; Reddles, P. W.; Gazzola, C.; Blakeley, R. L.; Zerner, B. *Can. J. Biochem.* **1980**, *58*, 1335.
(3) Jabri E.; Carr, M. B.; Hausinger, R. P.; Karplus, P. A.; *Science* **1995**, *268*, 998.
(4) Pearson, M. A.; Michel. L. O.; Hausinger, R. P.; Karplus, P. A. *Biochemistry* **1997**, *36*, 8164.
(5) Todd, M. J.; Hausinger, R. P. *Biol. Chem.* **1989**, *264*, 15835.
(6) Hase, J.; Kobashi, K. *J. Biochem (Tokyo)* **1967**, *62*, 293.
(7) Stemmler, A. J.; Kampf, J. W.; Kirk, M. L.; Pecoraro, V. L. *J. Am. Chem. Soc.* **1995**, *117*, 6368.

S0020-1669(97)01162-2 CCC: $15.00
Published on Web 06/15/1998

Scheme 1

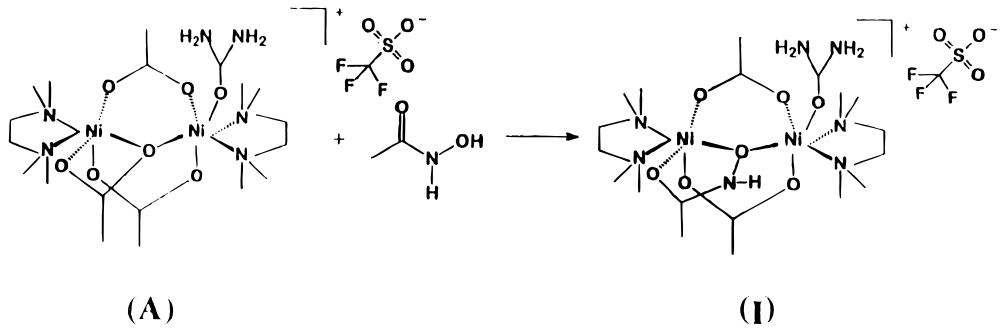

(A) **(I)**

Scheme 2

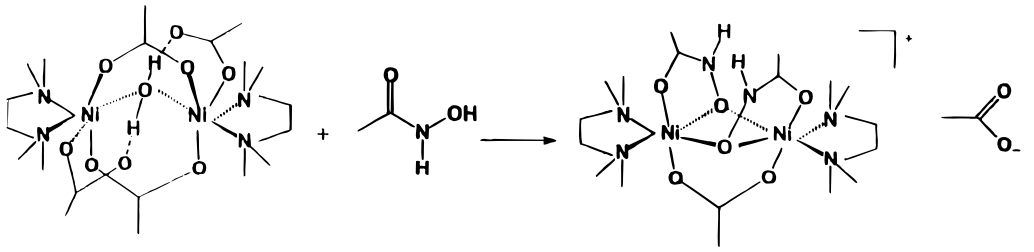

(B) **(II)**

In this paper, we report the synthesis of two dinuclear nickel complexes and containing one and two acetohydroxamate (AA) bridges, respectively. **I**, $[Ni_2(OAc)_2(AA)(urea)(tmen)_2][OTf]$, contains a single acetohydroxamate (AA) bridge with a Ni−Ni distance of 3.434(1) Å, very close to that in urease (3.5 Å),[3] and a urea molecule coordinated via its oxygen atom to one of the nickel centers (Figure 1) while **II**, $[Ni_2(OAc)(AA)_2(tmen)_2][OAc]$, contains two acetohydroxamate bridges with a Ni−Ni distance of 3.005(1) Å, considerably shorter than that of urease[3] (OAc, CH_3COO^-; tmen, *N*,*N*,*N*′,*N*′-tetramethylethylenediamine; OTf, CF_3SO_3; AHA, acetohydroxamic acid; AA, acetohydroxamate anion).

The structure of **I** is similar to that recently determined for the acetohydroxamate-inhibited C319A variant of *K. aerogenes* urease which shows replacement of three water molecules (Wat-500, Wat-501, and Wat-502) by a single hydroxamate bridge as in **I** and a Ni−Ni distance of 3.7 Å[8] but without, of course, a urea molecule coordinated to a nickel center.

Results and Discussion

The monobridged hydroxamate nickel dimer $[Ni_2(OAc)_2(AA)(urea)(tmen)_2][OTf]$ **(I)** was prepared by the reaction of acetohydroxamic acid and the dinuclear nickel urease model compound $[Ni_2(OAc)_3(urea)(tmen)_2][OTf]$ **(A)**,[9] in methanol (Scheme 1).

The dibridged acetohydroxamate complex **II**, $[Ni_2(OAc)(AA)_2(tmen)_2][OAc]$, was obtained as green crystals by reaction of acetohydroxamic acid and the dinuclear nickel complex $[Ni_2(OH_2)(OAc)_4(tmen)_2]$ **(B)**,[10] in a 2:1 molar ratio in methanol (Scheme 2). The analogous dibridged benzohydroxamate complex **III**, $[Ni_2(OAc)(BA)_2(tmen)_2][OAc]\cdot AcOH\cdot H_2O$ was obtained similarly by reaction of benzohydroxamic acid (BHA) and **B**.

In both cases, similar reactions occurred in dichloromethane as solvent. In the case of **II** and **III**, the products contain not only the acetate counterion but also a free acetic acid molecule and a free water molecule as shown analytically (see Experimental Section) and confirmed by the crystal structure (see Supporting Information). **II** may also be prepared directly by the reaction of nickel acetate tetrahydrate, tmen and AHA in methanol. In contrast to the reaction of **A** and **B** with AHA with formation of the singly and doubly bridged acetohydroxamate (AA) dimers **I** and **II**, respectively, reactions of **A** and **B** with glycine hydroxamic acid (GHA) in dichloromethane gave only the red mononuclear nickel complex, $Ni(GA)_2$, which contains the hydroxamate acting as an N,N donor.[11] Reaction of **A** and **B** with GHA in methanol gave only ill-defined brown solids. The inhibitory potency of a series of *N*-acylglycinohydroxamic acids has been reported.[12]

The electronic spectra of the four complexes, measured in dichloromethane **(A**, **B**, **I**, and **II)** are very similar and typical of a distorted octahedral oxygen environment about a Ni(II) center with bands in the three regions 1072−1093, 645−666, and 386−394 nm being assigned to the three spin-allowed transitions $^3A_{2g}(F) \rightarrow {}^3T_{2g}(F)$, $^3A_{2g}(F) \rightarrow {}^3T_{1g}(F)$, and $^3A_{2g}(F) \rightarrow {}^3T_{1g}(P)$ for an octahedral d^8 ion[13] (see Supporting Information).

The infrared spectra measured in KBr disks are most informative in the carbonyl region (see Table 1). Thus the peak at 1669 cm^{-1} in **I** is very close to that at 1670 cm^{-1} in the parent complex **A** in accord with the crystal structure data, which shows similar Ni−O (urea) distances in **A** and **I** (see below). However, the bridging acetates in **I** lie at higher frequencies than in **A** (1634 and 1621 $cm^{-1,}$ respectively) while the peak

(8) Hausinger, R. P., private communication.
(9) Wages, H. E.; Taft, K. L.; Lippard, S. J. *Inorg. Chem.* **1993**, *32*, 4985.
(10) Turpeinen, U.; Hämäläinen; Reedyk, J. *Polyhedron* **1987**, *6*, 1603.
(11) Brown, D. A.; Roche, A. L.; Pakkanen, T. A.; Pakkanen, T. T.; Smolander, K. *J. Chem. Soc., Chem. Commun.* **1982**, 3035.
(12) Munakata, K.; Kobashi, K.; Takebe, S.; Hase, J. *J. Pharmacobio-Dyn.* **1980**, *3*, 451.
(13) Figgis, B. N. *Introduction to Ligand Fields*; Interscience Publishers: New York, 1966.

Table 1. Infrared Spectroscopic Data for Complexes **A**, **B**, **I**, and **II**

medium	A	I	B	II	assignment
KBr	1669	1669			urea
	1621	1634	1635	1632	bidentate bridging acetate
		1607		1593	coordinated hydroxamate
	1553		1542		monodentate acetate
CH_2Cl_2	1664	1660			urea
	1617	1628	1624	1628	bidentate bridging acetate
		1614			monodentate hydroxamate
		1591		1593	coordinated hydroxamate
	1549	1543	1549	1548	monodentate acetate
acetone	1668	1667			urea
	1619	1630	1634	1630	bidentate bridging acetate
		1594		1594	coordinated hydroxamate
	1552	1546	1554	1543	monodentate acetate

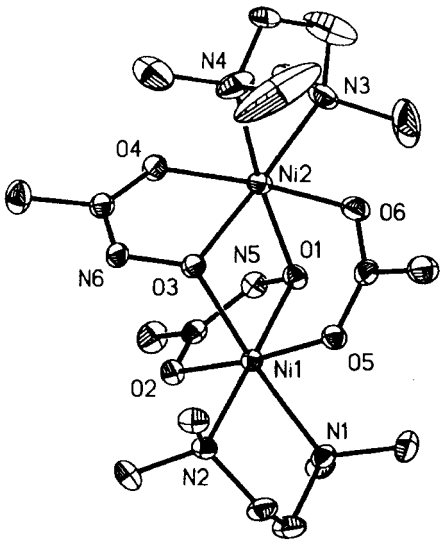

Figure 2. Molecular structure of the cation in compound **II** showing the labeling scheme. All hydrogens have been omitted for clarity.

of the unidentate/bridging acetate at 1553 cm^{-1} has disappeared. A new absorption at 1607 cm^{-1} in **I** is assigned to the coordinated carbonyl of the bridged hydroxamate, in good agreement with reported values for the monomeric bisacetohydroxamate complex, $Ni(AA)_2(H_2O)_2$.[14]

In the case of the dibridged product **II** formed from **B**, the bridging acetates in **B** have been replaced by a peak at 1632 cm^{-1} assigned to the remaining bridging acetate while the peaks for the two unidentate acetates in **B**, also H bonded to the bridging water, are replaced by a peak at 1593 cm^{-1} assigned similarly to the 1607 cm^{-1} peak in **I**, to the carbonyl function of the bridging acetohydroxamate groups bonded to the nickel atoms.

Crystal Structures of I and II

The structures of **I** and **II** are shown in Figures 1 and 2, respectively. Crystallographic data are given in Table 2, with selected bond distances and angles in Tables 3 and 4 for **I** and **II** respectively.

The ORTEP diagram of the cation **I** (Figure 1) shows that the monodentate bridging acetate in **A**, $[Ni_2(OAc)_3(urea)(tmen)_2][OTf]$, has been replaced by a bridging acetohydroxamate group in which the deprotonated hydroxyl oxygen (O_5) is bonded to both nickel atoms and the carbonyl oxygen (O_6) is bonded to only one nickel atom as in the previously reported doubly bridged salicylhydroxamate complex.[7] The urea remains coordinated via its oxygen atom to the other nickel atom. As a consequence of forming only a single acetohydroxamate bridge in **I**, the Ni−Ni distance of 3.434(1) Å (Table 3) is close to that in uninhibited urease, 3.5 Å,[3] and the parent compound **A**[9] and slightly less than that in the acetohydroxamate-inhibited C319A, 3.7 Å.[8] These distances are clearly longer than those observed in the doubly bridged salicylhydroxamate complex, 3.016 Å,[7] and the doubly bridged complex **II**, 3.005(1) Å, discussed below (Table 4). The coordination about the nickel atoms in **I** is distorted octahedral but less so than in the parent compound **A**; for example, O(3)−Ni(1)−O(5) in **I** is 94.72° whereas the equivalent O(1)−Ni(1)−O(4) in **A** is 103.42°. The Ni(1)−O(7)(urea) distance in **I** is slightly longer than that in **A** (2.0970(17) Å and 2.070(2) Å, respectively).

(14) Brown, D. A.; Roche, A. L. *Inorg. Chem.* **1983**, *22*, 2199.

Table 2. Crystal Data and Structure Refinement for Compounds **I** and **II**

	I	II
empirical formula	$C_{20}H_{46}F_3N_7O_{10}SNi_2$	$C_{22}H_{52}N_6O_{11}Ni_2$
M	751.12	694.08
cryst syst	monoclinic	orthorhombic
space group	$P2_1/c$	$P2_12_12_1$
a/Å	11.0157(3)	9.6885(6)
b/Å	13.6232(6)	13.0858(3)
c/Å	22.5156(3)	25.7459(12)
α/°	90	90
β/°	94.46	90
γ/°	90	90
V/Å^3	3368.7(2)	3264.1(2)
T/K	180(2)	180(2)
Z	4	4
λ/Å	0.710 73	0.710 73
ρ(calcd)/(Mg/m^3)	1.481	1.408
cryst size/mm	0.20 × 0.16 × 0.16	0.42 × 0.40 × 0.24
μ/mm^{-1}	1.252	1.213
hkl ranges	−8, 14; −18, 17; −29, 24	−12, 12; −14, 17; −34, 31
no. of data collected	19 605	20 580
indep reflns	7905 (R_{int} = 0.048)	7668 (R_{int} = 0.033)
max and min transm	0.802, 0.556	0.745, 0.619
$R(F)$ [$I > 2\sigma(I)$]	4.37%	3.92%
$R_w(F^2)$ (all data)	8.86%	9.63%
goodness of fit on F^2	0.953	1.030
largest peak and hole/e Å^{-3}	0.390, −0.482	0.706, −0.659
data, restraints, param	7905, 17, 446	7668, 1, 397

Table 3. Selected Bond Lengths (Å) and Angles (deg) for **I**

Ni(1)−Ni(2)	3.434(1)		
Ni(1)−O(1)	2.0440(18)	Ni(1)−O(3)	2.0480(18)
Ni(1)−O(5)	2.0577(18)	Ni(1)−O(7)	2.9070(17)
Ni(1)−N(2)	2.166(2)	Ni(1)−N(1)	2.195(2)
Ni(2)−O(2)	2.0169(19)	Ni(2)−O(5)	2.0455(18)
Ni(2)−O(6)	2.0550(19)	Ni(2)−O(4)	2.0550(19)
Ni(2)−N(3)	2.147(2)	Ni(2)−N(4)	2.182(2)
O(l)−Ni(1)−O(3)	92.72(7)	O(1)−Ni(1)−O(5)	92.91(7)
O(3)−Ni(1)−O(5)	94.72(7)	O(1)−Ni(1)−O(7)	176.27(7)
O(3)−Ni(1)−O(7)	90.19(7)	O(5)−Ni(1)−O(7)	89.18(7)
O(1)−Ni(1)−N(2)	86.96(8)	O(3)−Ni(1)−N(2)	90.56(8)
O(5)−Ni(1)−N(2)	174.72(8)	O(7)−Ni(1)−N(2)	90.68(8)
O(1)−Ni(1)−N(1)	89.87(8)	O(3)−Ni(1)−N(1)	173.50(9)
O(5)−Ni(1)−N(1)	91.10(8)	O(7)−Ni(1)−N(1)	86.99(8)
N(2)−Ni(1)−N(1)	83.62(9)	O(2)−Ni(2)−N(5)	94.00(7)
O(2)−Ni(2)−O(6)	175.01(8)	O(5)−Ni(2)−O(6)	81.08(7)
O(2)−Ni(2)−O(4)	91.70(8)	O(5)−Ni(2)−O(4)	97.17(7)
O(6)−Ni(2)−O(4)	88.14(8)	O(2)−Ni(2)−N(3)	92.00(9)
O(5)−Ni(2)−N(3)	172.74(8)	O(6)−Ni(2)−N(3)	92.97(9)
O(4)−Ni(2)−N(3)	86.72(9)	O(2)−Ni(2)−N(4)	87.30(9)
O(5)−Ni(2)−N(4)	92.29(8)	O(6)−Ni(2)−N(4)	93.67(9)
O(4)−Ni(2)−N(4)	170.53(9)	N(3)−Ni(2)−N(4)	83.91(10)

Table 4. Selected Bond Lengths (Å) and Angles (deg) for **II**

Ni(1)−Ni(2)	3.005(1)		
Ni(1)−O(5)	2.044(2)	Ni(1)−O(1)	2.057(2)
Ni(1)−O(2)	2.0684(19)	Ni(1)−O(3)	2.099(2)
Ni(1)−N(2)	2.121(3)	Ni(1)−N(1)	2.204(3)
Ni(2)−O(6)	2.031(2)	Ni(2)−O(3)	2.051(2)
Ni(2)−O(4)	2.075(2)	Ni(2)−O(1)	2.088(2)
Ni(2)−N(3)	2.127(3)	Ni(2)−N(4)	2.212(3)
O(5)−Ni(1)−O(1)	94.33(8)	O(5)−Ni(1)−O(2)	174.15(8)
O(1)−Ni(1)−O(2)	80.26(8)	O(5)−Ni(1)−O(3)	83.41(8)
O(1)−Ni(1)−O(3)	85.12(8)	O(2)−Ni(1)−O(3)	93.85(8)
O(5)−Ni(1)−N(2)	88.68(9)	O(1)−Ni(1)−N(2)	176.95(9)
O(2)−Ni(1)−N(2)	96.75(9)	O(3)−Ni(1)−N(2)	95.72(9)
O(5)−Ni(1)−N(1)	91.21(9)	O(1)−Ni(1)−N(1)	95.73(9)
O(2)−Ni(1)−N(1)	91.54(9)	O(3)−Ni(1)−N(1)	174.61(9)
N(2)−Ni(1)−N(1)	83.71(10)	O(6)−Ni(2)−O(3)	91.95(9)
O(6)−Ni(2)−O(4)	172.20(9)	O(3)−Ni(2)−O(4)	80.32(8)
O(6)−Ni(2)−O(1)	86.01(9)	O(3)−Ni(2)−O(1)	85.56(8)
O(4)−Ni(2)−O(1)	94.39(9)	O(6)−Ni(2)−N(3)	91.73(11)
O(3)−Ni(2)−N(3)	176.31(11)	O(4)−Ni(2)−N(3)	96.00(10)
O(1)−Ni(2)−N(3)	94.88(11)	O(6)−Ni(2)−N(4)	88.25(12)
O(3)−Ni(2)−N(4)	96.50(12)	O(4)−Ni(2)−N(4)	91.55(11)
O(1)−Ni(2)−N(4)	173.97(12)	N(3)−Ni(2)−N(4)	83.44(14)
N(5)−O(1)−Ni(1)	107.24(16)	N(5)−O(1)−Ni(2)	115.31(17)
Ni(1)−O(1)−Ni(2)	92.91(9)		

The ORTEP diagram of the cation of **II** (Figure 2) shows that in this case there is more disruption of the coordination environment of the dinuclear nickel center in **B**, $[Ni_2(OH_2)(OAc)_4(tmen)_2]$, on reaction with AHA than in the corresponding formation of **I** from **A**. Thus one of the bridging acetates, both terminal acetates, and the bridging water molecule in **B** have been replaced by two bridging acetohydroxamates bonded in a manner very similar to that in **I**, that is, utilizing the deprotonated hydroxamate oxygens, O(1) and O(3), as bridging atoms and carbonyl oxygens, O(2) and O(4), as monodentate atoms. Again both nickel atoms in **II** are in distorted octahedral environments in agreement with the UV/visible spectra; for example, the angle O(1)−Ni(1)−O(2) is 80.26° (Table 4).

The formation of two acetohydroxamate bridges in **II** results in a decrease in the Ni−Ni distance to 3.005(1) Å compared to 3.434(1) Å in the singly bridged complex **I,** but this value is close to that reported for the related dibridged salicyhydroxamate, $[Ni(Hshi)(H_2shi)(pyr)_4(OAc)]$ of 3.016 Å. This greater change in the structure of **II** from that of **B** compared to the change in **I** from **A** suggests that in **II** it is the presence of two bridging hydroxamates which largely determines the structure. Finally, it should be noted that the lattice of **II** contains not only the acetate counterion but also a displaced acetic acid molecule and a water molecule.

Magnetic Susceptibility Measurements. The temperature dependency of the molar susceptibilities and the effective magnetic moments of compounds **I**−**III** are shown in Figure 3. For all three complexes the effective magnetic moments increase with decreasing temperature. Such behavior can be referred to the presence of ferromagnetic exchange interaction between the Ni(II) centers. The effective magnetic moments run through a maximum and decrease at low temperatures. This behavior can be explained by a zero-field splitting of the $S = 2$ ground state of nickel ions. The $|2.0\rangle$ is the lowest lying state which causes the reduction of μ_{eff} at temperatures below 15 K. The room-temperature magnetic moments of 4.4−4.7 μ per nickel dimer are typical for nickel(II) ions in octahedral geometry.

For a quantitative description of the magnetic properties of the examined dinuclear compounds the data were fitted by using expression 1 for molar susceptibility versus temperature based

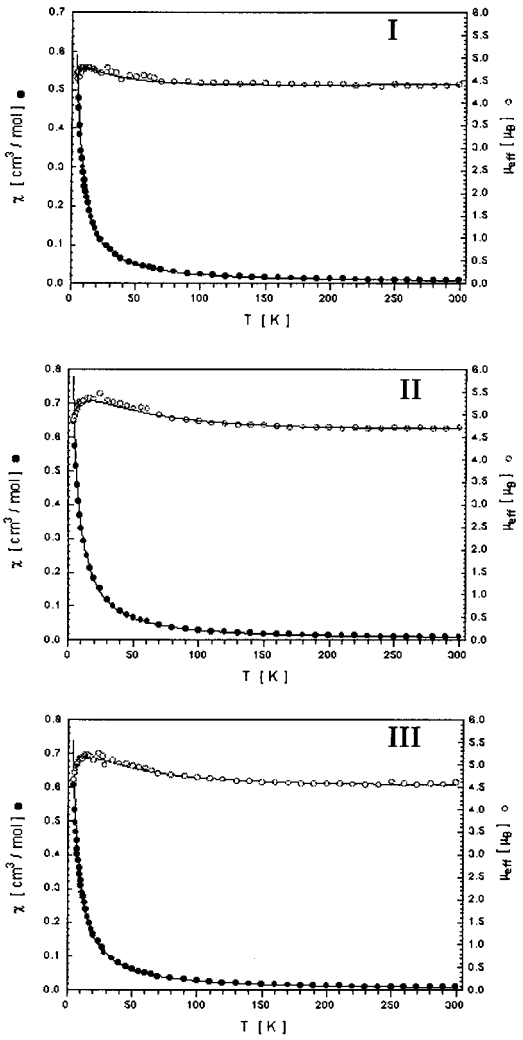

Figure 3. Temperature dependence of the molar susceptibility χ_m and the effective magnetic moment per dimer of **I**−**III**. The solid lines represent the best fitting of the data to eq 1.

on the isotropic Heisenberg−Dirac−van Vleck spin-exchange Hamiltonian:

$$H = -2J\mathbf{S}_1\cdot\mathbf{S}_2 \qquad (\mathbf{S}_1 = \mathbf{S}_2 = 1)$$

$$\chi(T) = (1 - x_p)\chi_{dim}(T) + 2x_p\chi_p(T) + 2N_\alpha \qquad (1)$$

with

$$\chi_{dim}(T) = \frac{N_A g^2 \mu_B{}^2}{k(T-\theta)} \frac{2e^{(2J/kT)} + 10e^{(6J/kT)}}{1 + 3e^{(2J/kT)} + 5e^{(6J/kT)}} \quad \text{and}$$

$$\chi_p(T) = \frac{N_A g^2 \mu_B{}^2}{3kT}$$

The Weiss constant θ was included to describe phenomenologically the decrease of the magnetic moments at low temperatures, which is equivalent to including a zero field splitting parameter D for the dinuclear unit, which would be more complicated. Due to the ferromagnetic coupling, it is not possible to determine accurately the paramagnetic impurity x_p, so this parameter has been fixed at 0. N_α refers to the temperature-independent paramagnetism, which is taken as 200×10^{-6} cm^3/mol per Ni(II) ion. The parameters obtained from the least-squares fits of the experimental data to eq 1 are given in Table 5.

Table 5. Fitted Parameters of Susceptibility Measurements of Compounds **I**−**III**

complex	J (cm^{-1})	g	θ (K)
I	4.09(25)	2.216(5)	−1.48(20)
II	11.65(10)	2.160(5)	0.73(5)
III	10.61(10)	2.131(5)	−0.74(5)

Nag and co-workers[15−17] have shown that for a series of octahedral and square pyramidal dinickel(II) complexes with centrosymmetric structures a linear relationship exists between the values of J and the Ni−O−Ni bridging angles wherein the inversion from ferromagnetic to antiferromagnetic coupling is anticipated at a bridging angle of 97°. This value is quite similar to the value found by Hatfield and co-workers[18] for hydroxy-bridged dinuclear copper(II) complexes. Exchange coupling in these compounds occurs only through the equatorial plane, in contrast to compounds **I**−**III,** which provide two different axial and equatorial pathways for exchange coupling. In addition, here the equatorial pathways involves two nonplanar nickel centers. Therefore, no magnetostructural relationship can be observed in this type of complex.

In the case of jack bean urease, temperature-dependent magnetic susceptibility measurements were initially interpreted in terms of antiferromagnetic coupling between the nickel(II) centers ($J = -6.3$ cm^{-1});[19] however, a subsequent saturation magnetization study provided no evidence for Ni−Ni exchange coupling.[20]

In contrast, the present series of hydroxamate-bridged nickel(II) complexes **I**−**III** and the related dibridged complex based on salicylhydroxamic acid[7] all exhibit ferromagnetic interaction (Table 5). It appears that replacement of acetate bridges in the parent compounds **A** and **B**, which are both antiferromagnetic,[9,10] by hydroxamate changes the interaction to ferromagnetic, which is considerably weaker for the monobridged hydroxamate complex **(I)** ($J \sim 4$ cm^{-1}) than for the dibridged hydroxamate complexes **II** and **III** ($J \sim 10$ cm^{-1}). The change from acetohydroxamate to benzohydroxamate has no significant influence on the magnetic properties. The inhibited urease of C319A variant contains only one bridging hydroxamate.[8]

Solution Studies

In view of the facile replacement of bridging carboxylate groups in **A** and **B** by the acetohydroxamate group, it is of interest to probe the mechanism of this reaction. Initially, attempts were made using infrared spectroscopy to monitor the reactions between A and AHA and B and AHA, but in all solvents studied these reactions were too fast to monitor; however, infrared spectroscopic studies were made of **A**, **B**, **I** and **II** in both dichloromethane and acetone and compared with those in KBr (Table 1). No decomposition of solutions **of A**, **B**, **I**, and **II** was observed in either solvent after 18 days at room temperature, so clearly they are stable in solution.

Results in CH_2Cl_2

The carbonyl region of **B** shows a peak at 1624 cm^{-1} assigned to a bridging acetate group and that at 1549 cm^{-1} assigned to the monodentate bridging acetate group. Similar peaks at 1617 and 1549 cm^{-1} occur for **A** with an additional peak at 1664 cm^{-1} assigned to the (O) coordinated urea molecule.[9] For both **A** and **B** the solution spectra are close to those in KBr.

Scheme 3. Carboxylate Shift

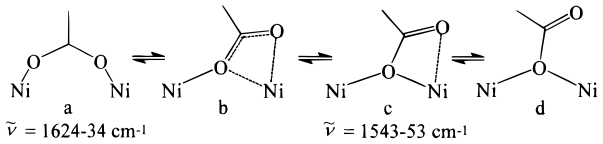

Scheme 4. Hydroxamate Shift

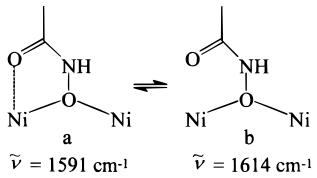

However, although **II** shows an expected peak at 1628 cm^{-1} due to a bridging acetate, it also shows a peak at 1593 cm^{-1} which is assigned to the coordinated hydroxamate by analogy with that observed in $Ni(AA)_2(H_2O)_2$[14] and, surprisingly, there is an additional peak at 1548 cm^{-1} which is absent in the KBr spectrum (Table 1). Similarly, while **I** shows analogous peaks at 1628 and 1591 cm^{-1} and a coordinated urea (O) peak at 1660 cm^{-1}, there is again a peak at 1543 cm^{-1} which is also absent in the KBr spectrum (Table 1). These peaks are typical of a monodentate acetate, which is clearly absent in the solid-state structures of **I** and **II** evidenced by their KBr spectra and crystal structures (Figures 1 and 2). We suggest that in certain solvents a bridging bidentate acetate (a, Scheme 3) is in equilibrium with the monodentate bridging intermediate (c, Scheme 3) in which there is only weak interaction between one of the carboxylate oxygen atoms and the nickel center. This is an example of the "carboxylate shift" invoked by Lippard et al. on examination of a range of carboxylate-bridged structures.[21] Thus in the crystal structures of **I** and **II** the equilibrium shown in Scheme 3 lies completely to the left whereas in certain solvents structure c occurs. The propensity for bridging carboxylates to undergo a carboxylate shift as suggested by the above infrared spectroscopic studies renders their replacement by hydroxamates remarkably facile. In view of the frequent occurrence of bridging carboxylates in metalloenzymes, this facile displacement may provide a clue to the observed inhibition of enzymes by hydroxamic acids.

In the case of **I** in CH_2Cl_2, a new peak occurs at 1614 cm^{-1} (Table 1) which lies intermediate in value between that of the free acetohydroxamic acid at 1621 cm^{-1} [14] and the O,O-coordinated species at 1589 cm^{-1}.[14] We suggest tentatively that this extra peak arises from an analogous "hydroxamate shift" (Scheme 4) in which the hydroxamate bridging group (a, Scheme 4) is in equilibrium with form b (Scheme 4) in which there is only a weak interaction between the hydroxamate carbonyl oxygen and a nickel center. The presence of an equilibrium was confirmed by variable-temperature infrared studies of **I** in CH_2Cl_2 when the peak at 1614 cm^{-1} was found to decrease in intensity over the range room temperature to −60 °C. Similar results were obtained in acetone.

(15) Nanda, K. K.; Thompson, L. K.; Bridson, J. N.; Nag, K. *J. Chem. Soc., Chem. Commun.* **1994**, 1337.
(16) Nanda, K. K.; Das, R.; Thompson, L. K.; Venkatsubramanian, K.; Nag, K. *Inorg. Chem.* **1994**, *33*, 1188.
(17) Nanda, K. K.; Das, R.; Thompson, L. K.; Venkatsubramanian, K.; Nag, K.; *Inorg. Chem.* **1994**, *33*, 5934.
(18) Crawford, V. H.; Richardson, H. W.; Wasson, D. J.; Hatfield, W. E. *Inorg. Chem.* **1976**, *15*, 2107.
(19) Clark, P. A.; Wilcox, D. E. *Inorg. Chem.* **1989**, *28*, 1326.
(20) Day, E. P.; Peterson, J.; Sendova, M. S.; Todd, M. J.; Hausinger, R. P. *Inorg. Chem.* **1993**, *32*, 634.
(21) Rardin, L. R.; Tolman, W. B.; Lippard, S. J. *New J. Chem.* **1991**, *15*, 417.

Experimental Section

Solvents were freshly purified by standard methods. Reagents were used directly without purification. Infrared spectra were measured as KBr disks on a Perkin-Elmer 1720FT spectrometer linked to a 3700 data station. UV/visible spectra were measured in dichloromethane solution on a Perkin-Elmer Lambda 6 UV/vis spectrometer. Low-temperature infrared studies were carried out using a Specac cell and control system.

Analyses were performed by the Microanalytical Unit of the Chemical Services Unit of University College, Dublin.

Preparation of Hydroxamic Acids. Acetohydroxamic acid, benzohydroxamic acid, and glycine hydroxamic acid were prepared as described previously.[14]

Preparation of Parent Dinuclear Nickel Complexes (A and B). Complex **B**, $[Ni_2(H_2O)(OAc)_4(tmen)_2]$, was prepared by the literature method[10] (yield, 97%). Complex **A**, $[Ni_2(OAc)_3(urea)(tmen)_2][OTf]$, was prepared from **B** by the literature method[9] (yield 40%).

Preparation of Monobridged Acetohydroxamate Complex (I), $[Ni_2(OAc)_2(AA)(urea)(tmen)_2][OTf]$. Complex **A** (736 mg, 1.00 mmol) and acetohydroxamic acid (AHA) (75 mg, 1.00 mmol) were dissolved in methanol (2 mL) and reacted for 30 min. Evaporation of the methanol gave an oil, which on solution in diethyl ether, centrifuging, and standing at room temperature for several hours deposited green crystals of **I** (yield, 0.530 mmol, 53%). Anal. Calcd for $Ni_2C_{20}H_{46}O_{10}N_7SF_3$ (**I**): C, 31.98; H, 6.17; N, 13.05; Ni, 15.63. Found: C, 31.85; H, 6.17; N, 12.93; Ni, 15.38.

Preparation of Dibridged Acetohydroxamate Complex (II), $[Ni_2(OAc)(AA)_2(tmen)_2][OAc]\cdot AcOH\cdot H_2O$. Complex **B** (302 mg, 0.500 mmol) and acetohydroxamic acid (75 mg, 1.00 mmol) were dissolved in methanol (1 mL) and reacted for 30 min. Workup as for **I** above gave green/blue crystals of **II** (yield, 0.486 mmol, 49%). Anal. Calcd for $Ni_2C_{22}H_{52}O_{11}N_6$ (**II**): C, 38.42; H, 7.34; N, 12.09. Found: C, 38.70; H, 7.53; N, 12.24.

Complex **II** can also be prepared by the direct reaction of stoichiometric amounts of nickel acetate tetrahydrate, tmen, and AHA in methanol. Similar reactions occurred between AHA and both **A** and **B** in CH_2Cl_2 as solvent.

Preparation of Dibridged Benzohydroxamate Complex (III), $[Ni_2(OAc)(BA)_2(tmen)_2]$ $[OAc]\cdot AcOH\cdot H_2O$. This was prepared by the same method as **II**, replacing AHA with BHA, to give green crystals (yield, 0.271 mmol, 54%). Anal. Calcd for $Ni_2C_{32}H_{56}O_{11}N_6$ **(III)**: C, 46.97; H, 6.85; N, 10.27. Found: C, 47.05; H, 6.92; N, 9.95.

Reactions of A and B with Glycine Hydroxamic Acid (GHA). Reaction of complexes **A** and **B** (1 mmol) with GHA (90 mg, 1 mmol) in dichloromethane (1 mL) with stirring for 2 h gave in both cases a red precipitate of $Ni(GA)_2$, which was centrifuged and dried with ether (yield, 90%). Anal. Calcd for $NiC_4H_{10}O_4$: C, 20.29; H, 4.26; N, 23.66. Found (reaction with **A**): C, 19.73; H, 4.24; N, 22.42. Found (reaction with **B**): C, 20.30; H, 4.29; N, 22.96.

Reaction of **A** and **B** with GHA in methanol gave brown solids of variable analyses.

Crystal Structure Determinations of Complexes (I) and (II). Crystals of both **I** and **II** suitable for X-ray analysis were obtained directly from the above preparation methods. Data were collected using a Siemens SMART CCD area-detector diffractometer. A full hemisphere of reciprocal space was scanned by a combination of three sets of exposures; each set had a different ϕ angle for the crystal, and each exposure of l0 s covered 0.3° in ω. The crystal to detector distance was 5.01 cm.

Crystal decay was monitored by repeating the initial frames at the end of the data collection and analyzing the duplicate reflections; for compounds **I** and **II** the decay was negligible. A multiscan absorption correction was applied using SADABS.[22]

The structure was solved by direct methods using SHELXTL-PC[23] and refined by full-matrix least squares on F^2 for all data using SHELXL-97.[24] Hydrogen atoms were added at calculated positions and refined using a riding model. Anisotropic temperature factors were used for all non-H atoms; H atoms were given isotropic temperature factors equal to 1.2 (or 1.5 for methyl hydrogens) times the equivalent isotropic displacement parameter of the atom to which the H atom is attached.

Magnetic Measurements. The magnetic susceptibilities of powdered samples of **I, II**, and **III** were recorded on a Faraday-type magnetometer consisting of a Cahn RG electrobalance, a Leyboldt Heraeus VNK 300 helium flux cryostat, and a Bruker BE25 magnet connected with a Bruker B-Mn 200/60 power supply in the temperature range 4.5−300 K. The applied magnetic field was about 0.5 T. Details of the apparatus have been described elsewhere.[25,26] The experimental susceptibility data were corrected for underlying diamagnetism in the usual manner using Pascal's constants.[27] Corrections for diamagnetism were estimated as -376.9, -353.9, and -447.2×10^{-6} cm^3/mol for **I**, **II**, and **III**, respectively.

Conclusions

The above structural comparisons, between **A** and **I** and between **B** and **II**, show that an acetohydroxamate group (AA) can replace both a bridging acetate group and bridging acetate−water groups with relatively small changes in structure. Although the coordination environments of the nickel centers in urease, which are distorted trigonal pyramidal and pseudotetrahedral, respectively,[3] appear to be different from the octahedral coordination of the nickel centers in **I** and **II** (and **A** and **B**), when account is taken of the additional water molecules, Wat-501 and Wat-502 in urease,[4] the environments are comparable; moreover, it should be noted that in the acetohydroxamate-inhibited C319A variant, replacement of the three water molecules by one bridging acetohydroxamate has occurred.[4] The solution studies show that replacement of bridging acetates by hydroxamates is very rapid and that in certain solvents bridging acetates undergo carboxylate shifts, which increases their lability.

In view of the frequent occurrence of both carboxylate groups and water molecules as structural features of metalloenzymes, the ready replacement of these groups by acetohydroxamate in the model dinuclear nickel complexes, **A** and **B**, may provide a clue to the observed inhibition of enzymes by hydroxamic acids.

Acknowledgment. We are pleased to acknowledge the support of the EUCOST program, Project D8/0010/97.

Supporting Information Available: Tables of electronic spectra, crystallographic data, atomic coordinates and equivalent isotropic displacement parameters, bond lengths and angles, and anisotropic displacement parameters for **I** and **II** (13 pages). Ordering information is given on any current masthead page.

IC9711628

(22) Sheldrick, G. M. *SADABS, Empirical Absorption Corrections Program*; University of Göttingen, Göttingen, Germany, 1997.

(23) Siemens. SHELXTL-PC Version 5.0 Reference Manual; Siemens Industrial Autom., Inc., Analytical Instrumentation: Madison, WI, 1994.

(24) Sheldrick, G. M. *SHELXL-97 Program for Crystal Structure Refinement*; University of Göttingen: Göttingen, Germany, 1997.

(25) Merz, L.; Haase, W. *J. Chem. Soc., Dalton Trans.* **1980**, 875.

(26) Gehring, S.; Fleischhauer; Paulus, H.; Haase, W. *Inorg. Chem.* **1993**, *32*, 54.

(27) Kahn, O.; *Molecular Magnetism*; VCH Publishers: New York, 1993.